Exciton–erbium interactions in Si nanocrystal-doped SiO_2

P. G. Kik[a] and A. Polman
FOM Institute for Atomic and Molecular Physics, Kruislaan 407, 1098 SJ Amsterdam, The Netherlands

(Received 3 May 2000; accepted for publication 18 May 2000)

The presence of silicon nanocrystals in Er doped SiO_2 can enhance the effective Er optical absorption cross section by several orders of magnitude due to a strong coupling between quantum confined excitons and Er. This article studies the fundamental processes that determine the potential of Si nanocrystals as sensitizers for use in Er doped waveguide amplifiers or lasers. Silicon nanocrystals were formed in SiO_2 using Si ion implantation and thermal annealing. The nanocrystal-doped SiO_2 layer was implanted with different doses of Er, resulting in Er peak concentrations in the range 0.015–1.8 at. %. All samples show a broad nanocrystal-related luminescence spectrum centered around 800 nm and a sharp Er luminescence line at 1536 nm. By varying the Er concentration and measuring the nanocrystal and Er photoluminescence intensity, the nanocrystal excitation rate, the Er excitation and decay rate, and the Er saturation with pump power, we conclude that: (a) the maximum amount of Er that can be excited via exciton recombination in Si nanocrystals is 1–2 Er ions per nanocrystal, (b) the Er concentration limit can be explained by two different mechanisms occurring at high pump power, namely *Auger de-excitation* and *pair-induced quenching*, (c) the excitable Er ions are most likely located in an SiO_2-like environment, and have a luminescence efficiency $<18\%$, and (d) at a typical nanocrystal concentration of $10^{19}\,cm^{-3}$, the maximum optical gain at 1.54 μm of an Er-doped waveguide amplifier based on Si nanocrystal-doped SiO_2 is $\sim$0.6 dB/cm. © *2000 American Institute of Physics.* [S0021-8979(00)06516-6]

I. INTRODUCTION

Erbium-doped optical amplifiers are an important component in optical telecommunication networks. The operation of these amplifiers relies on an optical transition of Er^{3+} at 1.54 μm, which is in the region of optimum transmission of silica based glass fiber. The transition responsible for the 1.54 μm luminescence occurs within the partially filled $4f$ shell of Er^{3+}, which is electrically shielded from its surroundings by filled $5s$ and $5p$ shells. As a result of spin–spin and spin–orbit interactions, the $4f$ shell can be optically excited into several discrete energy levels, for example at 0.81, 0.98, and 1.54 μm. The optical cross sections for these transitions are small, typically on the order of $10^{-21}\,cm^2$, because optical transitions between the $4f$ levels are parity forbidden. Consequently, rather high pump intensities are needed to reach population inversion, typically on the order of 1 kW/cm^2.

Several years ago, it was shown that Er incorporated in silicon-rich SiO_2 could also be excited outside of the Er^{3+} optical absorption lines.[1,2] The same effect was observed in Er-doped porous silicon,[3,4] which consists of silicon nanoclusters surrounded by a thin layer of SiO_2, and more recently in Si nanocrystal-doped SiO_2 containing Er.[5–9] It was shown that the addition of Si nanocrystals to Er-doped SiO_2 strongly enhances the effective Er absorption cross section. We have recently demonstrated that exciton recombination inside Si nanocrystals causes the excitation of Er through a strong coupling mechanism.[10]

This energy transfer process could enable the fabrication of an optical amplifier operating at 1.54 μm that is optically excited at pump intensities as low as a few milliwatts per millimeter squared. Additionally, it may be possible to excite Er electrically by supplying electrical carriers to an Er and Si nanocrystal-doped SiO_2 layer. However, little is known about a number of crucial parameters that determine the performance of such devices, such as the Er excitation efficiency, the Er luminescence efficiency, and the maximum Er concentration.

In our previous work[10] we have already shown that at high Er concentration (1.8 at. %) the Er excitation process is efficient (quantum efficiency $>55\%$), while the excitable fraction of the Er is low. In the present article we report the Er concentration dependence of the optical properties of Si nanocrystal-doped SiO_2. We show that the maximum concentration of excitable Er in this material is $\sim$0.02 at. %, and propose mechanisms that could give rise to this concentration maximum. Furthermore, we show that the Er luminescence efficiency is less than 18%. Finally, we show that the maximum gain that can be obtained in this material is $\sim$0.6 dB/cm at 1.54 μm.

II. EXPERIMENT

A 100 nm thick layer of SiO_2 was grown on a lightly *B*-doped Si(100) substrate by means of wet thermal oxidation. This layer was implanted with 35 keV Si to a dose of $6\times10^{16}\,cm^{-2}$. The implantation yields an approximately Gaussian depth distribution of excess Si in the SiO_2 film, with a peak concentration of 19 at. % at a depth of 45 nm.

[a]Electronic mail: Kik@amolf.nl

 © 2000 American Institute of Physics

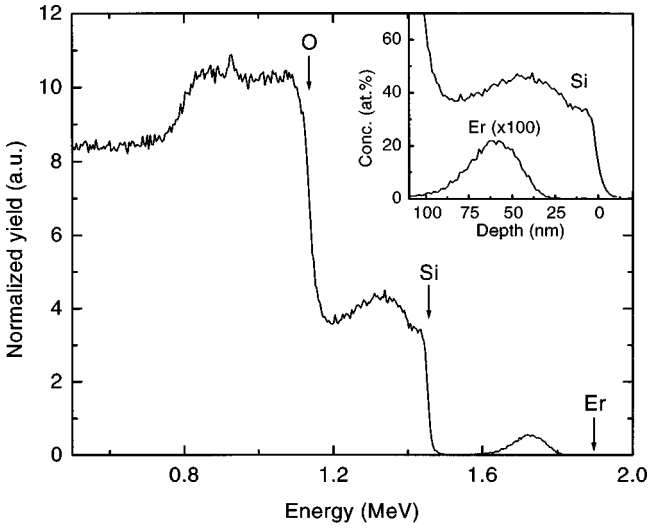

FIG. 1. RBS measurement of Si nanocrystal-doped SiO_2 implanted with 4.5×10^{14} Er/cm^2, taken at a scattering angle of 96.2° using a 2 MeV He^+ beam. The surface energies of Er, Si, and O are indicated by the arrows. The inset shows the corresponding Er and Si concentration profiles.

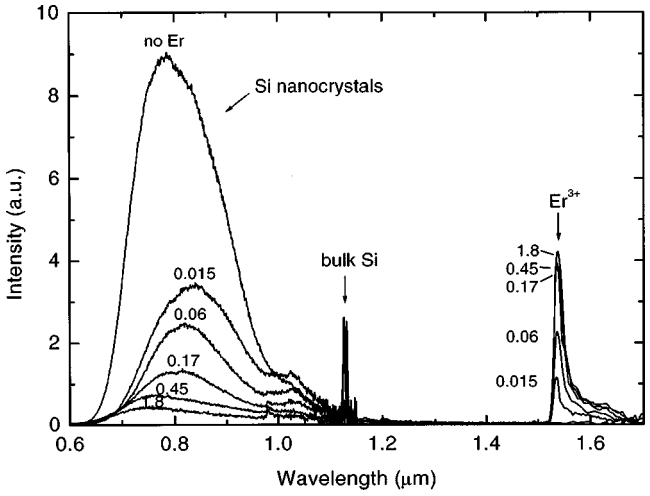

FIG. 2. Photoluminescence spectra of Si nanocrystal-doped SiO_2 containing different Er concentrations in the range of 0–1.8 at. %, measured at 15 K using a pump power of 1 mW at 458 nm.

The samples were subsequently annealed at 1100 °C for 10 min in vacuum at a base pressure below 3×10^{-7} mbar, in order to induce nucleation and growth of Si nanocrystals. This treatment has been shown to produce Si nanocrystals with a diameter in the range of 2–5 nm.[10,11] Assuming a typical nanocrystal diameter of 3 nm ($\sim10^3$ Si atoms), the nanocrystal peak concentration is estimated to be $\sim10^{19}$ cm^{-3} at the center of the SiO_2 layer. The samples were then implanted with different Er doses in the range 3.6×10^{13}–5.1×10^{15} cm^{-2} at a fixed energy of 125 keV. These implants result in an approximately Gaussian Er depth distribution, with Er peak concentrations ranging from 0.015 to 1.8 at. % at a depth of 61 nm. A non-Er-implanted sample was kept as a reference. Figure 1 shows a Rutherford backscattering spectrometry (RBS) measurement of a sample containing 4.5×10^{14} Er/cm^2 taken at a scattering angle of 96.2° using a 2.0 MeV He^+ beam. The energies corresponding to erbium, silicon, and oxygen located at the sample surface are indicated. Note that the rise of the RBS signal around 1.13 MeV is the combined effect of signal from oxygen at the sample surface and signal from silicon in the substrate. The inset shows the Si and Er concentration profile in the SiO_2 layer as obtained from the RBS data. Note that the Er ions were implanted slightly deeper than the Si ions.

All samples were annealed for 10 min in vacuum at 1000 °C to remove implantation-induced damage. In order to further reduce defect-related luminescence and to saturate dangling bonds on the Si nanocrystal surface, a passivating anneal was performed at 780 °C for 30 min. in forming gas (H_2:N_2 at 1:9) at atmospheric pressure.

Photoluminescence (PL) spectra were measured using the 458 nm line of an Ar laser as excitation source at a peak power of 1 mW in a $\sim$1 mm^2 laser spot. The laser beam was modulated *on–off* at 11 Hz using an acousto-optical modulator. The emitted light was passed through a grating monochromator and detected using standard lock-in techniques. Spectra were measured in the range 600–1150 nm using a AgOCs photomultiplier tube (PMT), and in the range 1100–1700 nm using a liquid-nitrogen cooled Ge detector. All spectra were corrected for the system response. Photoluminescence decay traces were recorded using a multichannel photon counting system in combination with the PMT and a digitizing oscilloscope in combination with the Ge detector. The system response for the two cases was 150 ns and 160 μs, respectively. For all luminescence measurements the samples were cooled to 15 K using a closed-cycle He cryostat.

III. RESULTS AND DISCUSSION

A. Photoluminescence versus Er concentration

Figure 2 shows a PL spectrum of an SiO_2 film doped with Si nanocrystals (marked ''no Er''). The sample shows a broad luminescence band peaking at 790 nm. We have previously shown that this luminescence is caused by the radiative recombination of electron–hole pairs (excitons) confined within the Si nanocrystals.[11] Due to quantum confinement[12] the exciton luminescence appears at energies above the band gap energy of bulk Si (1.17 eV at 15 K). The large spectral width of the nanocrystal luminescence is the result of the broad nanocrystal size distribution (2–5 nm diameter). The luminescence peak at 1.13 μm is caused by phonon-assisted electron–hole pair recombination in the Si substrate. Figure 2 also shows luminescence spectra for samples containing Er at various concentrations. The incorporation of 0.015 at. % Er reduces the nanocrystal luminescence by more than a factor two, and a luminescence peak appears at a wavelength of 1.536 μm. This wavelength corresponds to the radiative transition from the first excited state ($^4I_{13/2}$) to the ground state ($^4I_{15/2}$) of Er^{3+}. Increasing the Er concentration leads to a further reduction of the nanocrystal luminescence intensity, accompanied by an increase of the Er luminescence intensity. This behavior is consistent with the strong coupling model,[10] in which a nanocrystal becomes ''dark'' once it couples to a nearby Er ion. Increasing the Er concentration therefore increases the fraction of dark nanocrystals.

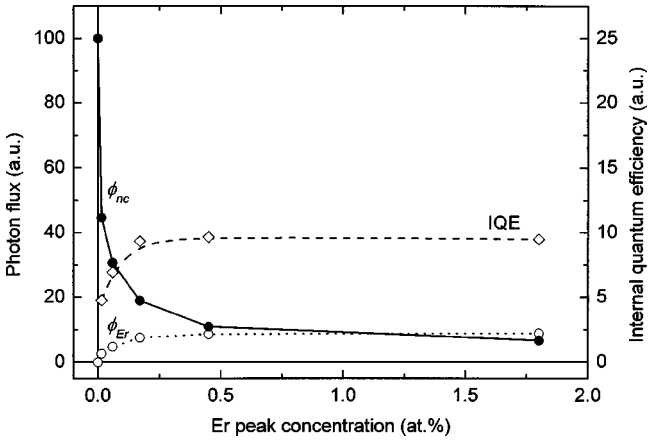

FIG. 3. Integrated emission of the nanocrystal-related luminescence (●) and the Er-related luminescence (○) on the same relative scale, measured at 15 K. The relative internal quantum efficiency of the Er excitation process is plotted on the right hand axis (◇).

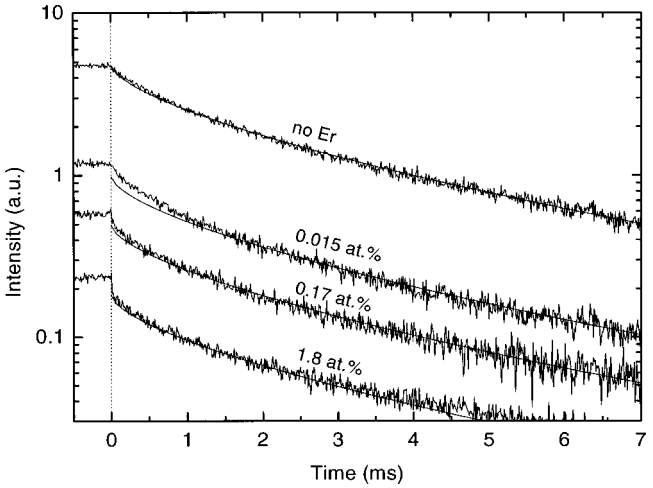

FIG. 4. Photoluminescence decay traces of the nanocrystal luminescence at 750 nm for different Er concentrations in the range of 0–1.8 at. %, measured at 15 K using 1 mW pump power at 458 nm. The pump is switched off at $t=0$. The drawn lines represent stretched exponential decay with $\tau=2.0$ ms and $\beta=0.65$.

Upon increasing the Er concentration, the nanocrystal luminescence spectrum is first seen to shift to longer wavelength, and then to shorter wavelength. This effect is related to the slight mismatch in the Er and Si implantation depth (see Fig. 1). We have shown in our previous work[13] that the long-wavelength emission originates from relatively large nanocrystals located at the center of the Si implanted region, while the emission at short wavelength originates from relatively small nanocrystals located in the tails of the Si concentration profile. Since in the present work the Er is implanted slightly deeper than the silicon, the incorporation of a small amount of Er will first affect the (small) nanocrystals near the SiO_2/Si interface, leading to a reduction in the emission at short wavelength. As the Er concentration is increased, the (large) nanocrystals at the center of the SiO_2 film are also affected, leading to a reduction in the emission at large wavelength, as observed in Fig. 2.

B. Internal quantum efficiency versus Er concentration

The power conversion efficiency of potential optical amplifiers or lasers making use of Er excitation via Si nanocrystals will depend on the internal quantum efficiency (IQE) of the energy transfer process, i.e., the efficiency with which nanocrystals coupled to Er can generate excited Er. To determine the Er concentration dependence of the IQE, the intensities in Fig. 2 were converted to photon flux and then integrated over the nanocrystal emission spectrum and the Er emission spectrum, respectively. Figure 3 shows the thus obtained nanocrystal related emission ϕ_{nc}(●) and Er related emission ϕ_{Er}(○) on the same relative scale. At zero Er concentration $\phi_{Er}=0$ and $\phi_{nc}=100$. At the highest Er concentration $\phi_{Er}=9$ and $\phi_{nc}=7$, which indicates that nine Er-related photons are obtained at the cost of 93 nanocrystal-related photons. These values give a *relative* measure of the concentration dependent IQE, since we do not know the Er and nanocrystal luminescence efficiencies. Thus we have

$$\mathrm{IQE} \propto \frac{\phi_{\mathrm{Er}}}{\phi_{\mathrm{nc}}(0)-\phi_{\mathrm{nc}}}, \tag{1}$$

with $\phi_{nc}(0)$ the nanocrystal-related emission at zero Er concentration. This IQE is depicted in Fig. 3 for all Er concentrations (◇). The IQE first increases with Er concentration, and then saturates above 0.2 at. % Er. The fact that the internal quantum efficiency reaches a fixed value at a high Er concentration confirms that the observed reduction in nanocrystal luminescence is caused by energy transfer to Er and not, for example, by the destruction of nanocrystals during the ion implantation process. We conclude that the IQE of nanocrystals coupled to Er is essentially independent of the Er concentration. The relatively low efficiency at low Er concentration will be discussed further in Sec. III F.

Using independent measurements of the nanocrystal and Er excitation rates published previously,[10] we have shown that at an Er concentration of 1.8 at. %, the IQE$\geqslant$55%. The observation in Fig. 3 that only 10% of the nanocrystal photons yield 1.54 μm photons then implies that the Er luminescence efficiency from the first excited state $\eta_{1.54}<18\%$. Implications of this observation will be discussed in Sec. III G.

C. Nanocrystal luminescence lifetime versus Er concentration

Figure 4 shows nanocrystal luminescence decay traces taken at 750 nm and $T=15$ K for samples containing different Er concentrations. In a sample containing no Er, the nanocrystal luminescence shows a 1/*e* lifetime of 2.0 ms. The decay is well described by stretched exponential decay of the form $I(t)=\exp(-(t/\tau)^{\beta})$ with $\tau=2.0$ ms and $\beta=0.65$ (solid line). The same curve has been overlaid on all data in order to facilitate comparison between the different traces.

Incorporation of Er leads to a significant reduction of the nanocrystal luminescence intensity at 750 nm, as was already observed in Fig. 2. The decay time, however, varies only slightly from sample to sample and no trend is observed with

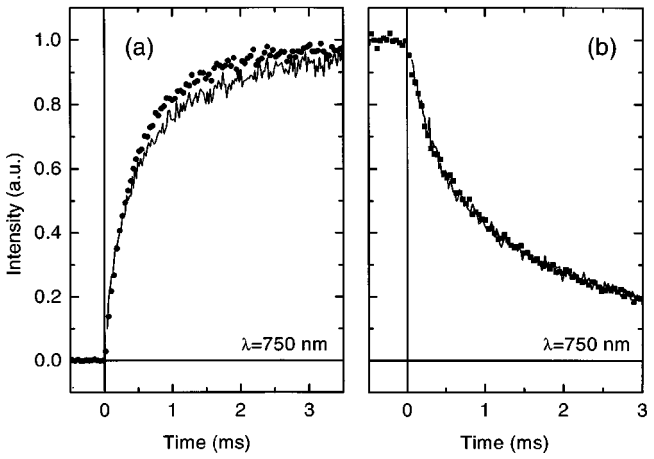

FIG. 5. Photoluminescence rise (a) and decay traces (b) of the nanocrystal luminescence at 750 nm, measured at 15 K using 5 mW excitation at 458 nm.

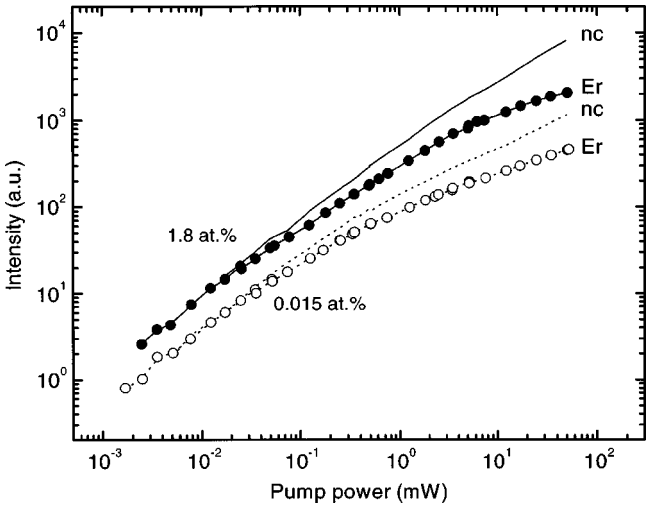

FIG. 6. Photoluminescence intensity of the nanocrystal luminescence and the Er luminescence as a function of pump power for samples containing 0.015 and 1.8 at. % Er, measured at 15 K using 458 nm pump light in a ~1 mm^2 spot.

increasing Er concentration. The highest Er concentration sample shows a small initial fast decay, which is attributed to luminescence from defects in the SiO_2 matrix.[13]

These lifetime measurements confirm the strong-coupling model,[10] which states that the Er induced intensity decrease in Fig. 2 is due to a reduction in the number of luminescent nanocrystals. All remaining nanocrystal luminescence therefore originates from nanocrystals that are not coupled to Er, which show their intrinsic decay characteristics. These nanocrystals are expected to be mostly located near the sample surface where the Er concentration is relatively low (see RBS data in Fig. 1).

The fact that the nanocrystal luminescence decay time does not depend on the Er concentration has been observed previously by Franzò *et al.*[9] They explained their experimental findings by assuming that the nanocrystal-related luminescence around 750 nm is not emitted by quantum confined excitons, but rather by a luminescent center at the nc–Si/SiO_2 interface that is excited via optically generated excitons. In this scenario, excitons can transfer their energy either to such a center or to an Er ion, after which the Er ion and the center do not interact. Consequently, varying the Er concentration would only shift the balance between these two processes, and indeed leave the lifetime of the 750 nm luminescence unaffected. However, according to this model, the reduction of the nanocrystal luminescence in Fig. 2 should be accompanied by a reduction of the apparent nanocrystal *excitation rate*. Such a reduction is not observed, as will be shown below.

The effect of Er on the nanocrystal excitation rate was measured by monitoring the time dependence of the 750 nm luminescence while modulating the pump beam. Figure 5 shows normalized luminescence traces at 750 nm after switching the pump laser on (a) and off (b) for a sample containing no Er (dots) and a sample containing an Er peak concentration of 1.8 at. % (solid line). The applied pump power was 5 mW at 458 nm. The defect related fast component (see Fig. 4) has been removed from the data to facilitate comparison. The nanocrystal luminescence decay characteristics [Fig. 5(b)] are identical for the two samples, with a $1/e$ decay time $\tau_{decay}=1.30$ ms. This is somewhat shorter than the $1/e$ times observed at a pump power of 1 mW, possibly due to exciton–exciton interactions or saturation of nanocrystals with a long lifetime. The $1/e$ rise times τ_{rise} are 0.47 and 0.56 ms for samples containing no Er and 1.8 at. % Er.

The measured τ_{rise} and τ_{decay} can be used to determine the excitation rate R_{exc}. If we model the luminescence at 750 nm by a two-level system, R_{exc} is given by

$$\frac{1}{\tau_{rise}} = R_{exc} + \frac{1}{\tau_{decay}}. \tag{2}$$

This gives a nanocrystal excitation rate of 1360 s^{-1} at 750 nm in the sample containing no Er. Incorporation of 1.8 at. % Er reduces the nanocrystal excitation rate to 1020 s^{-1}. The 25% reduction in excitation rate is insufficient to explain the observed twentyfold decrease of the nanocrystal luminescence intensity at 750 nm upon incorporating 1.8 at. % Er (Fig. 2). Hence the data cannot be described using the model proposed by Franzò *et al.*. The data can be described by the strong coupling model,[10] since this mechanism indeed leaves the luminescence characteristics of the luminescent nanocrystals, i.e., those which are not coupled to Er, unaffected.

D. Er luminescence intensity versus pump power

The data in Fig. 3 show a sublinear increase of the Er intensity with concentration. This can be ascribed to the fact that as the Er concentration is increased, the exciton concentration available for Er excitation is reduced. At sufficiently high pump power, however, the Er luminescence intensity is no longer limited by the exciton concentration but rather by the total amount of excitable Er. Therefore we can compare the total amount of excitable Er in samples with different Er concentrations by comparing Er luminescence intensities at high pump power.

Figure 6 shows the effect of pump power on the Er and nanocrystal luminescence intensity for samples containing 0.015 and 1.8 at. % Er, respectively. For both samples the

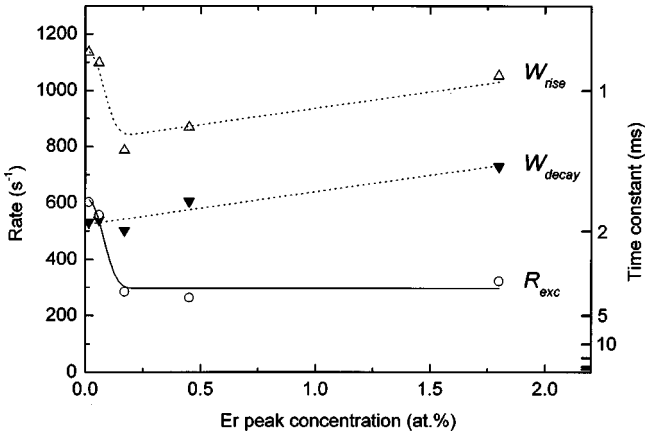

FIG. 7. Rise times (△) and decay times (▼) of the 1.536 μm Er luminescence, measured at 15 K using a pump power of 1 mW at 458 nm, and the Er excitation rate derived from these data (○). The drawn lines serve as a guide to the eye.

nanocrystal luminescence intensity was scaled to coincide with the low-power Er luminescence intensity. Below 20 μW the Er luminescence and the nanocrystal luminescence depend linearly on pump power. At these low pump powers the Er luminescence intensities from the two samples differ by a factor ~2. Increasing the pump power produces a sublinear increase of the Er luminescence in both samples, suggesting that a significant fraction of the excitable Er is brought into the first excited state. At a pump power of 50 mW the nanocrystal luminescence continues to increase, while the Er luminescence intensity levels off. In this pump power regime the exciton generation rate is no longer the limiting factor for the Er luminescence intensity. Nevertheless, the Er luminescence intensities for the two samples at 50 mW pump power differ by only a factor of 5, even though the total amount of Er in the samples differs by more than a factor of 100.

The above shows that the concentration of excitable Er in the high concentration (1.8 at.%) sample is at most 5 times higher than in the low concentration (0.015 at.%) sample. This suggest that the concentration of excitable Er is $<$0.1 at.%. The existence of such a concentration limit is also observed in the Er excitation rate, as will be shown in the following paragraph.

E. The Er excitation and decay rate versus Er concentration

When the amount of Er coupled to a nanocrystal is increased, the Er excitation rate per ion should reduce since several Er ions then compete for the same exciton. In order to determine the concentration dependent Er excitation rate we performed rise time and decay time measurements of the Er luminescence at 1.536 μm. At the applied pump power of 1 mW all samples show approximately exponential time dependencies. Figure 7 shows the measured rates $W_{\mathrm{rise}}=1/\tau_{\mathrm{rise}}$(△) and $W_{\mathrm{decay}}=1/\tau_{\mathrm{decay}}$(▼) obtained by exponential fitting of the data.

The Er decay rate increases from 500 to 700 s^{-1} as the Er peak concentration is increased from 0.015 to 1.8 at.%. This increase is attributed to a concentration quenching effect which is known to occur when rare earth ions are spaced closely enough to allow for energy exchange between neighboring ions. As a result, excitation energy can migrate[14] to neighboring ions, which may in turn be coupled nonradiatively to quenching sites, e.g., defects or OH groups present in the matrix. In a simple concentration quenching model the Er decay rate increases linearly with Er concentration, which is indeed observed in Fig. 7. By measuring the slope of the decay rate data in Fig. 7, we can estimate[15] that the concentration of quenching sites in the Er implanted Si nanocrystal-doped SiO_2 film is as low as 10^{18} cm^{-3}.

Data for the Er excitation rate R_{exc} calculated from τ_{rise} and τ_{decay} using Eq. (2) are also shown in Fig. 7 (○). At an Er concentration of 0.015 at.%, the Er excitation rate is 600 s^{-1}. Increasing the Er concentration to 0.17 at.% reduces the excitation rate by a factor of 2. A further increase of the Er concentration has no effect on the excitation rate, even though at these concentrations several Er ions might couple to the same nanocrystal, which would reduce the excitation rate per Er ion. The fact that such a reduction is not observed shows that there is an upper limit to the number of Er ions that can be excited by a single nanocrystal. From the data in Fig. 7 it is clear that this limit is reached at an Er concentration $<$0.17 at.% Er, which is consistent with the maximum value of 0.1 at.% Er found in the preceding paragraph.

From the measured Er excitation rate of ~300 s^{-1} at 1 mW we can determine an effective absorption cross section σ_{eff} for the Er excitation process. We find that $\sigma_{\mathrm{eff}} \approx 10^{-15}$ cm^2 at 458 nm, which is approximately a factor of 10^6 larger than what can be achieved using direct optical pumping of the Er ions. This value is of the same order as a typical Si nanocrystal absorption cross section at this wavelength,[16] confirming that a single nanocrystal can excite only a limited number of Er ions. In fact, in our previous work[10] we measured both the Er excitation rate at 1.536 μm and the nanocrystal excitation rate at 750 nm in a sample containing 1.8 at.% Er, and found that the Er excitation rate was a factor ~2 lower than the nanocrystal excitation rate. This proves that in the high Er concentration limit a single nanocrystal can excite only 1–2 Er ions. This observation, together with the estimated nanocrystal concentration of 10^{19} cm^{-3}, implies that the maximum excitable Er concentration is approximately 0.02 at.%.

It is intriguing to note that the Er excitation rate in the low concentration limit is approximately a factor of two higher than in the high concentration limit. This suggests that increasing the Er concentration either increases the number of excitable Er ions per nanocrystal from 1 to 2, or decreases the number of nanocrystals that can excite the same Er ion from 2 to 1.

The higher Er excitation rate at low concentration is also reflected in the pump power dependent Er luminescence intensity in Fig. 6. At high pump power, where the number of Er ions determines the luminescence intensity, the intensity from the high concentration sample is approximately 5 times higher than that from the low concentration sample. At low pump power, where the Er excitation rate is the limiting factor for the intensity, the intensity from the low concentra-

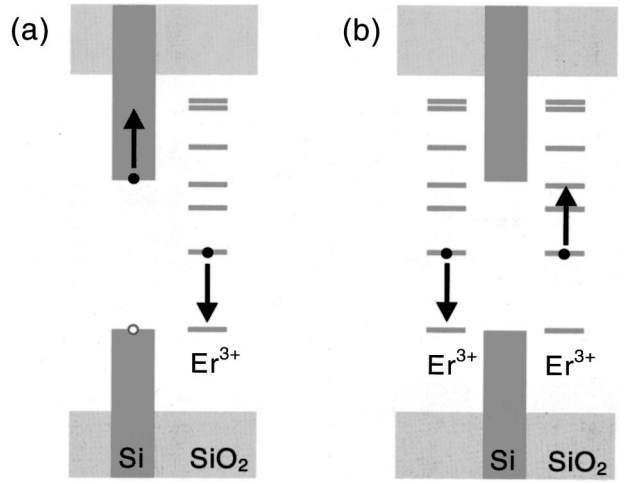

FIG. 8. Schematic band diagram of Er and Si nanocrystal-doped SiO_2 showing the process of (a) Auger de-excitation and (b) pair-induced quenching. These processes can account for the observed Er concentration limit in Si nanocrystal-doped SiO_2. Note that the Er energy levels represent collective states of the Er^{3+} $4f$ electrons, which are in fact well below the SiO_2 valence band edge.

tion sample is relatively higher by a factor ~2.5, as was expected from the higher excitation rate at low Er concentration.

F. Models describing the Er concentration limit

The existence of an upper limit to the amount of excitable Er could indicate that there is a limit to the amount of *optically active* Er that can be incorporated in this material. This may, for example, be caused by Er clustering or $ErSi_2$ formation at the Si/SiO_2 interface which would prevent the Er from being in the 3+ valence state. However, measurements on Er and Si nanocrystal-doped waveguides show a strong Er^{3+} related absorption,[17] suggesting that a large fraction of the Er is in the optically active state.

Alternatively, the observed concentration limit could be an intrinsic property of the excitation process. The amount of excitable Er will be low when the effective Er excitation efficiency is influenced by the presence of *excited* Er. Such a situation arises when the formation of an exciton near an excited Er ion immediately leads to (a) *Auger de-excitation*, in which the already excited Er ion transfers its energy to the generated exciton [Fig. 8(a)]. This process has been shown to occur in Er-doped bulk Si.[18] After such Auger de-excitation the exciton can relax and subsequently excite an Er ion, effectively bringing the system back to the situation before the exciton was formed. (b) *pair-induced quenching*. At sufficiently high Er concentration, two excited Er ions can interact yielding one Er ion in the $^4I_{9/2}$ state, which rapidly decays to the first excited state, and one Er ion in the ground state [Fig. 8(b)]. This cooperative upconversion effect usually produces a shortening of the Er decay rate at high pump powers, which has not been observed. However, if the Er–Er coupling is sufficiently strong, no effect on the lifetime is seen. This special case is usually called pair-induced quenching. An interesting point to note is that both of these processes reduce the internal quantum efficiency at high excitation rates. Figure 7 showed that at 1 mW pump power the Er excitation rate is relatively large at low Er concentrations. Consequently, the internal quantum efficiency is expected to be relatively low at low Er concentration, which is indeed observed in Fig. 3.

G. The Er local environment

The maximum Er lifetime in these Si nanocrystal-doped SiO_2 films is approximately 2 ms, corresponding to a decay rate of 500 s^{-1}. This decay rate is much higher than the radiative decay rate in pure SiO_2, which is ~50 s^{-1} (Ref. 19). The relatively fast decay can be caused by two effects, namely by additional nonradiative decay (W_{nr}) or by an increased radiative decay rate (W_r). We will now discuss the influence of these two effects in our samples. From the measurements in Fig. 3 we find that the Er luminescence efficiency $\eta_{1.54}<18\%$ (see Sec. III B). The luminescence efficiency is given by $\eta_{1.54}=W_r/(W_r+W_{nr})$. Since we know that the total decay rate W_r+W_{nr} is 500 s^{-1} (Fig. 7), we estimate that the Er radiative decay rate $W_r<90\,s^{-1}$. In fact, we expect the radiative decay rate to be higher than in bulk SiO_2 because of the presence of the Si substrate. If an ion is placed sufficiently close to a region with a high refractive index its radiative decay rate increases due to an increase of the local optical density of states (LDOS).[20] We have calculated the LDOS as a function of depth in a 100 nm SiO_2 film on Si, and assuming a radiative lifetime in bulk SiO_2 of 50 s^{-1}, we find that W_r increases smoothly from 50 s^{-1} at the sample surface to 120 s^{-1} near the SiO_2/Si interface. This corresponds quite well with the radiative decay rate $W_r<90\,s^{-1}$ obtained from our experiments. The fact that the observed decay rates can be described using the radiative lifetime in SiO_2 suggests that the excitable Er ions are not located inside the Si nanocrystals but in an SiO_2-like environment near the nanocrystals.

H. Device implications

In Sec. III E it was found that the effective Er absorption cross section σ_{eff} at 458 nm is approximately $10^{-15}\,cm^2$. This large cross section could be used in Er-doped waveguide lasers and amplifiers, in which population inversion is reached at low pump power. It is important to mention here that although all luminescence measurements in this article were performed at 15 K, we have previously shown[10] that the effective Er cross section is temperature independent up to at least 300 K.

In a Si nanocrystal sensitized optical amplifier based on the material studied in this article, the Er concentration should be kept low since we have shown that only ~0.02 at. % Er can be simultaneously kept in the excited state. At higher Er concentrations a large fraction of the Er will be in the ground state due to the processes discussed in Sec. III F, which will result in significant losses at 1.54 μm. The maximum gain per unit length $g_{\max}$ that can be achieved in a waveguide amplifier is given by $g_{\max}(\text{dB/cm})=4.34\times\sigma_{\text{em}}\times N_{\text{Er}}$ with N_{Er} the Er concentration and σ_{em} the emission cross section at 1.54 μm. Taking a typical value[21]

$\sigma_{em}=7\times10^{-21}\,cm^2$ and the maximum Er concentration ($2\times10^{19}\,Er/cm^3$) we find a maximum gain of 0.6 dB/cm.

In order to achieve net amplification at 1.54 μm, the Er induced gain should overcome the intrinsic device losses, including background absorption, scattering losses, and free carrier absorption. The latter process deserves special attention because the presence of electron–hole pairs in the amplification medium is *required* for the Er excitation process. In free carrier absorption free electrons and holes are excited higher in their respective energy bands by incoming photons. This process can occur at sub-bandgap energies and can therefore affect the 1.54 μm transmission.

In bulk silicon free carrier absorption cross sections at 1.54 μm are on the order of $10^{-17}\,cm^2$ (Ref. 22), which is $\sim10^4$ times larger than the cross section for stimulated emission of Er at 1.54 μm. Consequently, the exciton concentration in an Er-doped optical amplifier should be at least a factor 10^4 lower than the excited Er concentration. This means that at a typical nanocrystal pump rate of $10^3\,s^{-1}$ the exciton lifetime should be well below 0.1 μs. The achievement of net optical gain thus requires that the Er excitation and the nonradiative processes listed in Sec. III F occur within 0.1 μs. Furthermore, the concentration of nanocrystals *not* coupled to Er should be kept low since they show room-temperature exciton lifetimes >10 μs. The above shows that the achievement of optical gain requires careful optimization of the Er distribution. If the Er concentration is too low some nanocrystals will not be coupled to Er and these will induce free carrier absorption. If the Er concentration is too high part of the Er cannot be excited which will introduce loss at 1.54 μm. These narrow concentration limits suggest that stochastic methods for Er incorporation, such as ion implantation and sputtering, are not desirable. A more promising method would be chemical synthesis, in which the number of Er ions per nanocrystal can be accurately tuned.

In order to investigate the processes of optical gain and free carrier absorption in Er and Si nanocrystal-doped SiO_2, we have recently fabricated optical waveguides using Si nanocrystal-doped SiO_2 as the guiding medium. In these structures, the index contrast with the SiO_2 cladding is provided by the high-index Si nanocrystals. Preliminary transmission measurements on these samples show good optical mode confinement and clear Er related absorption at 1.54 μm.

IV. CONCLUSIONS

We have shown that the maximum amount of Er that can be excited via exciton recombination in Si nanocrystals is 1–2 Er ions per nanocrystal, corresponding to $\sim$0.02 at. % Er. This observation can be explained by two different mechanisms occurring at high pump power, namely Auger de-excitation and pair-induced quenching. The luminescent Er ions are most likely located in an SiO_2-like environment near the Si nanocrystals, and have a luminescence efficiency $\eta_{1.54}<18\%$. Using the obtained parameters we can predict a maximum optical gain of 0.6 dB/cm at 1.54 μm for a Si nanocrystal sensitized Er-doped waveguide amplifier in SiO_2, provided that free carrier absorption can be suppressed.

ACKNOWLEDGMENTS

This work is part of the research program of the Foundation for Fundamental Research on Matter (FOM) and was financially supported by the Netherlands Foundation for Scientific Research (NWO), the Dutch Technology Foundation (STW), and the SCOOP program of the European Union. The authors would like to thank M. de Dood for the optical mode density calculations.

[1] S. Lombardo, S. U. Campisano, G. N. van den Hoven, A. Cacciato, and A. Polman, Appl. Phys. Lett. **63**, 1942 (1993).
[2] G. N. van den Hoven, J. H. Shin, A. Polman, S. Lombardo, and S. U. Campisano, J. Appl. Phys. **78**, 2642 (1995).
[3] T. Kimura, A. Yokoi, H. Horiguchi, R. Saito, T. Ikoma, and A. Sato, Appl. Phys. Lett. **65**, 983 (1994).
[4] J. H. Shin, G. N. van den Hoven, and A. Polman, Appl. Phys. Lett. **66**, 2379 (1995).
[5] M. Fujii, M. Yoshida, Y. Kanzawa, S. Hayashi, and K. Yamamoto, Appl. Phys. Lett. **71**, 1198 (1997).
[6] M. Fujii, M. Yoshida, S. Hayashi, and K. Yamamoto, J. Appl. Phys. **84**, 4525 (1998).
[7] J. St. John, J. L. Coffer, Y. Chen, and R. F. Pinizzotto, J. Am. Chem. Soc. **121**, 1888 (1998).
[8] C. E. Chryssou, A. J. Kenyon, T. S. Iwayama, C. W. Pitt, and D. E. Hole, Appl. Phys. Lett. **75**, 2011 (1999).
[9] G. Franzò, V. Vinciguerra, and F. Priolo, Appl. Phys. A: Mater. Sci. Process. **69**, 3 (1999).
[10] P. G. Kik, M. L. Brongersma, and A. Polman, Appl. Phys. Lett. **76**, 2325 (2000).
[11] M. L. Brongersma, A. Polman, K. S. Min, E. Boer, T. Tambo, and H. A. Atwater, Appl. Phys. Lett. **72**, 2577 (1998).
[12] C. Delerue, G. Allan, and M. Lannoo, Phys. Rev. B **48**, 11 024 (1993).
[13] M. L. Brongersma, A. Polman, K. S. Min, and H. A. Atwater, J. Appl. Phys. **86**, 759 (2000).
[14] W. J. Miniscalco, J. Lightwave Technol. **9**, 234 (1991).
[15] F. Auzel, in *Radiationless Processes*, edited by B. DiBartolo (Plenum, New York, 1980).
[16] D. Kovalev, J. Diener, H. Heckler, G. Polisski, N. Künzner, and F. Koch, Phys. Rev. B **61**, 4485 (2000).
[17] P. G. Kik and A. Polman (unpublished).
[18] F. Priolo, G. Franzò, S. Coffa, and A. Carnera, Phys. Rev. B **57**, 4443 (1998).
[19] L. H. Slooff, M. J. A. de Dood, A. van Blaaderen, and A. Polman, Appl. Phys. Lett. **76**, 3682 (2000).
[20] H. P. Urbach and G. L. J. A. Rikken, Phys. Rev. A **57**, 3913 (1998).
[21] W. J. Miniscalco, J. Lightwave Technol. **9**, 234 (1991).
[22] M. A. Green, *Silicon solar cells* (University of New South Wales, Sydney, 1995).